# Kinetic Study on the Sulfuric Acid-Catalyzed Conversion of d -Galactose to Levulinic Acid in Water

Martina, Angela; Van De Bovenkamp, Henk H.; Noordergraaf, Inge W.; Winkelman, Jozef G.M.; Picchioni, Francesco; Heeres, Hero J.

*Published in:*
Industrial and Engineering Chemistry Research

*DOI:*
10.1021/acs.iecr.2c00706



*Publication date:*
2022

I&EC research
Industrial & Engineering Chemistry Research

pubs.acs.org/IECR

Article

# Kinetic Study on the Sulfuric Acid-Catalyzed Conversion of D-Galactose to Levulinic Acid in Water

Angela Martina, Henk H. van de Bovenkamp, Inge W. Noordergraaf, Jozef G. M. Winkelman, Francesco Picchioni, and Hero J. Heeres*

Cite This: *Ind. Eng. Chem. Res.* 2022, 61, 9178−9191

Read Online

ACCESS | Metrics & More | Article Recommendations | Supporting Information

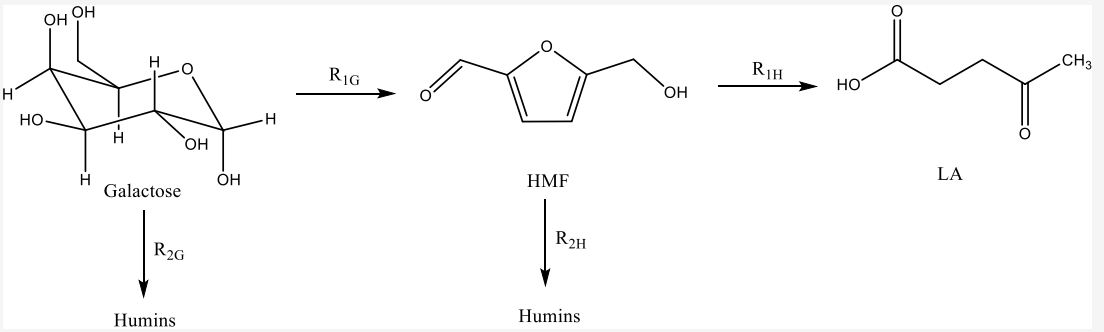


**ABSTRACT:** Levulinic acid is an interesting building block for biofuel (additives) and biobased chemicals. It is accessible by an acid-catalyzed reaction of a wide variety of carbohydrates. We here report a kinetic study on the conversion of D-galactose to levulinic acid in aqueous solutions with sulfuric acid as the catalyst. The experiments were carried out in a broad range of temperatures (140−200 °C), initial concentrations of galactose (0.055−1.110 M), and concentrations of sulfuric acid (0.05−1 M). The experimental data were modeled using a power-law approach, and good agreement between the experimental data and the model was obtained. The maximum yield of levulinic acid (54 mol %) was achieved at 130−140 °C, low initial galactose concentrations (0.055 M), and high acid concentrations (1 M). With the kinetic information available, the most suitable reactor configuration was determined, and it is predicted that a continuously stirred-tank reactor is preferred over a plug-flow reactor. The findings presented here may also be applicable to the kinetic modeling of levulinic acid synthesis from more complex biomass sources such as lignocellulosic (woody) and aquatic (e.g., seaweed) biomass.



## 1. INTRODUCTION

Research on green chemicals from biomass resources is of great interest to reduce the use of fossil resources and to green up the current petrochemical industry. Marine biomass (e.g., macroalgae or seaweed) is an attractive renewable source for producing chemicals and fuels due to its high growth rate as well as high carbohydrate and low lignin contents.[1] A comprehensive review on carbohydrates from seaweed[2] highlighted that seaweed is rich in C5-sugars (arabinose (ARA) and xylose (XYL)) and C6-sugars (glucose (GLU), galactose (GAL), and mannose (MAN)). The most abundant polysaccharides in red seaweeds are agars and carrageenans, which consist of GAL, sulfated-GAL, and 3,6-anhydrogalactose units with $\beta$-(1 → 4) and $\alpha$-(1 → 3) linkages; see Figure 1.

Our research activities involve the acid-catalyzed hydrolysis of marine biomass into valuable biobased chemicals. An interesting option is the conversion of marine biomass into 5-hydroxymethyl furfural (HMF) and levulinic acid (LA) by acid treatment. HMF is a furan derivative with an aldehyde and alcohol groups, which has been widely investigated due to its high potential to serve as a platform chemical to produce polymer precursors like 2,5-dicarboxylic acid (FDCA), formic acid, 2,5-dimethylfuran, and levulinic acid (LA).[3]

LA is a versatile building block that contains a ketone group and a carboxylic acid, allowing multiple conversion strategies. It is considered a precursor for biofuels and various biobased chemicals (see the SI, Figure S1); well-known examples are $\gamma$-valerolactone, 2-methyltetrahydrofuran, and $\alpha$-angelicalactone.[4,5]

The synthesis of LA from various sugars (GLU, fructose (FRC), GAL, XYL, MAN) has been reported, and HMF is usually identified as the main intermediate.[6−10] Previous studies on the conversion of GAL to HMF (either as the

**Received:** March 2, 2022
**Revised:** May 19, 2022
**Accepted:** May 19, 2022
**Published:** June 22, 2022

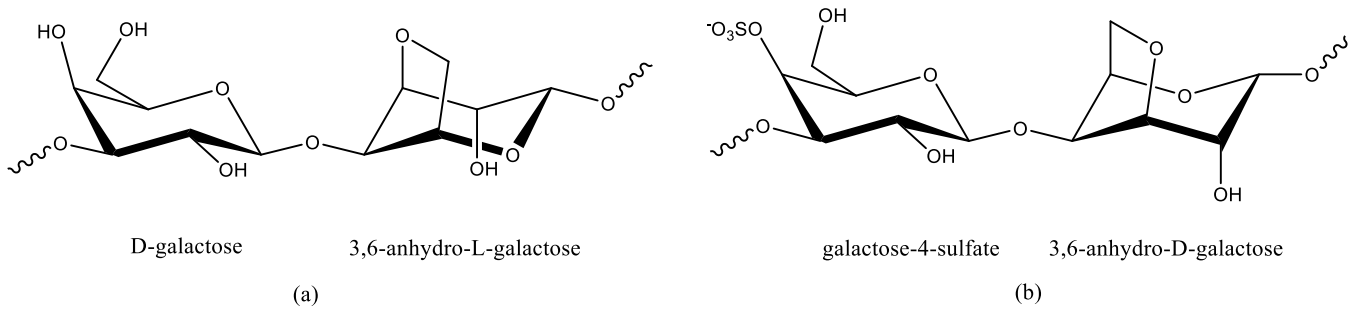


**Figure 1.** Agarose (a) and κ-carrageenan (b).

main product or the intermediate in LA synthesis) and LA are provided in Table 1.

Two representative studies have been reported in water using either sulfuric acid ($H_2SO_4$) or methanesulfonic acid (MSA) as the catalyst (Table 1, entries 1 and 2). LA yields were <30 mol % for sulfuric acid and 40 mol % for MSA. HMF yields in water at these conditions are below 2.5 mol %, indicating that GAL is not a good carbohydrate source for HMF synthesis. As such, it fits with the general trend that ketoses (like FRC) are better for HMF synthesis than aldoses when using water as the solvent. Other identified byproducts were 1,6-anhydro-α-D-galactofuranose and dihydroxyacetone (DHA).[7,9] A number of studies have been performed in organic solvents like DMF/DMSO and ionic liquids, with the main objective to increase HMF yields (Table 1, entries 3−7). Here, both Bronsted and Lewis acids have been used as catalysts, either homogeneous or heterogeneous in nature. The best results regarding HMF yield (33 mol %) were obtained by Binder et al. (Table 1, entry 6).

Kinetic studies on the conversion of C5-sugars and C6-sugars, especially GLU and FRC, to HMF and LA using an acid catalyst in aqueous solutions have been reported.[6,8,16,17] The available kinetic studies using GAL as the feed and water as the solvent are summarized in Table 2.

Kinetic studies on the conversion of GAL in aqueous solutions are typically performed in batch reactors using inorganic Bronsted acid catalysts ($H_2SO_4$, HCl, $H_2SO_3$, $H_3PO_4$, and $C_4H_8O_2$) with reaction temperatures between 120 and 210 °C.[18−20] The only exceptions are the last two entries in Table 2. The study by Liu et al. involves an acid bisulfite pretreatment of Douglas fir chips followed by enzymatic hydrolysis with GAL as one of the intermediates. Khajavi et al. explored the degradation kinetics of various monosaccharides (including GAL) using subcritical water as a reaction solvent. Most of the kinetic models only include the rate of GAL, ignoring other reactions in the network (e.g., HMF and humin formation).

Saeman explored the kinetics for wood (Douglas fir) saccharification, focusing on cellulose and GLU hydrolysis in dilute $H_2SO_4$ at 170−190 °C (Table 2). As part of this study, XYL, ARA, MAN, and GAL were also studied independently and converted in 0.8% $H_2SO_4$ at 180 °C to determine the relative decomposition rate of the individual sugars. The reaction was modeled assuming a first-order reaction in sugar, and the reaction rate constant (k) of GAL was found to be 0.0273 $min^{-1}$ with a half-life period of 26.4 min. The degradation of GAL appeared to be slightly faster than that of GLU ($k$ = 0.0241 $min^{-1}$, half-life = 28.6 min). The reactions were carried out at a single temperature, and thus, the activation energies were not reported.[18]

A kinetic study on the hydrothermal decomposition of lignocellulose was reported by Baugh and McCarty;[19] see Table 2 for details. Pseudo-first-order models were developed for the conversion of XYL, MAN, GLU, GAL, 2-furfural, and HMF over a pH range of 1−4 and temperatures between 170 and 230 °C. The activation energies of the conversion of XYL, GAL, and MAN to products were estimated to be 141, 138, and 134 $kJ·mol^{-1}$, respectively.

Shi *et al.* explored various inorganic Bronsted acids such as $H_2SO_4$, HCl, and $H_2SO_3$ for the conversion of ARA, XYL, MAN, GLU, and GAL in a batch system at 120−140 °C.[20] A first-order dependency in sugar was assumed. The activation energies of GAL in HCl, $H_2SO_4$, and $H_2SO_3$ systems were found 141.6, 147.5, and 148.3 $kJ·mol^{-1}$, respectively.

Liu *et al.* studied the kinetics of sugar formation (ARA, GAL, GLU, XYL, MAN) and byproducts (HMF, furfural, acetic acid) from an acid bisulfite pretreatment followed by enzymatic hydrolysis of Douglas fir[21] in batch setups. After acid treatment at 135−155 °C for 20−180 min, the pretreated solids were then hydrolyzed for 72 h using enzymes (CTech2 and HTech2). The Saeman model[18] was applied to obtain the reaction rate constant. The activation energies of lignocellulosic biomass hydrolysis to GAL (93.5 $kJ·mol^{-1}$) and GAL conversion to products (73.1 $kJ·mol^{-1}$) were calculated using the Arrhenius equation.

Apart from the batch system, a continuous flow setup using subcritical water (10 MPa, 180−260 °C) as the solvent was used to study the conversion rate of monosaccharides at these conditions.[22] An adopted Weibull model was used to model the experimental data set. The activation energy of GAL degradation (170 $kJ·mol^{-1}$) was higher than reported by Baugh and McCarty (138 $kJ·mol^{-1}$).

When considering the state of the art as given above, a kinetic model for the conversion of GAL to LA including the kinetics of HMF as an intermediate and humin as a byproduct has not been reported to date. We here report an experimental and modeling study on the acid-catalyzed decomposition of GAL to LA in an aqueous solution using $H_2SO_4$ as the catalyst. The effects of process conditions (temperature, initial GAL concentration, $H_2SO_4$ concentration) on the reaction rate were determined. A kinetic model was set up, and the relevant kinetic parameters for the individual reactions in the network were calculated. The model uses the power-law approach, which is rationalized by the fact that the main purpose of this work is to obtain a kinetic model to be used for reactor design and scale-up, and for this purpose, the power-law approach is well suited. The optimum conditions to obtain the highest yield of LA in the batch reactor were determined based on the model.



https://doi.org/10.1021/acs.iecr.2c00706
Ind. Eng. Chem. Res. 2022, 61, 9178−9191

Table 1. Overview of Relevant Studies on the Conversion of GAL to HMF and LA[a]

| entry | catalyst | solvent | temperature (°C) | reaction time (min) | yield | ref |
|---|---|---|---|---|---|---|
| 1 | $H_2SO_4$ | water | 150 | 30−600 | <2.5 mol % HMF 30 mol % LA | 7 |
| 2 | MSA | water | 130−210 | 10−50 | 0.7−40.3 mol % LA | 11 |
| 3 | Amberlyst-70 | ethanol/water | 175 | 120 | <3 mol % HMF <30 mol % LA | 9 |
| 4 | HT, Amberlyst-15 | DMF | 100−120 | 180 | 15.1−21.3% HMF[b] | 12 |
| 5 | $LaCl_3$ | DMSO | 120 | 120 | 6.7% HMF[b] | 13 |
| 6 | $H_2SO_4$, $CrCl_2$, $CrCl_3$, $CrBr_3$, $Cr(NO_3)_3$ Additives: LiCl, LiBr | [EMIM]Cl, DMA, DMSO | 120 | 120−180 | 1−33 mol % HMF[b] | 14 |
| 7 | $[NMP][HSO_4]$ $[NMP][HSO_4]$ $[C_3SO_3HMIM][HSO_4]$ Additive: $CoCl_2$ | [AMIM]Cl [BMIM]Cl | 120 | 60 | 3.7−19.7 mol % HMF[b] | 15 |

[a]MSA, methanesulfonic acid; HT, hydrotalcite; DMF, *N*,*N*-dimethylformamide; DMSO, dimethyl sulfoxide; DMA, dimethylacetamide; [EMIM]Cl, 1-ethyl-3-methylimidazolium chloride; [AMIM]Cl, 1-allyl-3-methylimidazolium chloride; [BMIM]Cl, 1-butyl-3-methylimidazolium chloride; $[NMP][HSO_4]$, *N*-methyl-2-pyrrolidonium hydrogen sulfate; $[C_3SO_3HMIM][HSO_4]$, 1-(4-sulfonic acid)-propyl-3-methylimidazolium hydrogen sulfate. [b]LA yields are not provided.

## 2. EXPERIMENTAL SECTION

**2.1. Chemicals.** All chemicals were used without further purification. Galactose (GAL, 99%) [CAS: 59-23-4] was purchased from Acros Organics. $H_2SO_4$ (95−97%) [7664-93-9] was purchased from Boom. HMF (99%) [67-47-0] and formic acid, FA (≥95%) [64-18-6], were obtained from Sigma-Aldrich. LA (98%) [123-76-2] was purchased from Alfa Aesar. Milli-Q water was used to prepare the solutions.

**2.2. Experimental Procedures.** The experimental procedures are based on a procedure given by Girisuta et al.[8] The acid-catalyzed hydrolysis reaction was carried out in glass ampoules (length of 15 cm, internal diameter of 3 mm, and wall thickness of 1.5 mm). The ampoules were filled with approximately 0.3 mL of the solution consisting of GAL (0.055−1.110 M) and $H_2SO_4$ (0.05−1 M). The ampoules were sealed with a torch. A series of ampoules was placed in an aluminum rack and placed in a GC oven (Hewlett Packard 5890A) at a specified temperature (140−200 °C). At certain reaction times, an ampoule was taken from the oven and directly quenched into an ice-water bath to stop the reaction. The ampoules were then opened, and the reaction mixture was taken out. The mixture was filtered using a 0.45 $\mu$m PTFE filter to remove any insoluble materials. The clear solution was analyzed using high-performance liquid chromatography (HPLC). At the start of a hydrolysis reaction, the reaction occurs nonisothermally due to the heating up of the glass ampoule and its content from room temperature to the oven temperature. To compensate for this nonisothermal behavior in the kinetic modeling studies, the temperature inside the ampoules as a function of time during the heating-up process was determined experimentally. Based on the experiment, 3−5 min is needed to heat up the ampoule and its content from room temperature to the oven temperature (see the SI Section S5).

**2.3. Analytical Methods.** The liquid phase composition was determined using an Agilent 1200 HPLC system equipped with an Agilent 1200 pump, a Bio-Rad organic acid column (Aminex HPX-87H), a refractive index detector, and an ultraviolet detector. Aqueous sulfuric acid (5 mM) was used as the mobile phase at a flow rate of 0.55 mL $min^{-1}$. The HPLC column was operated at 60 °C. The analysis for a sample was complete in 45 min. The concentration of each individual compound (GAL, HMF, FA, and LA) in the reaction product mixture was determined using calibration curves obtained by analyzing standard solutions with known concentrations. A typical HPLC chromatogram is shown in the SI (Figure S2). Besides the main components, several small peaks are also present, which are from intermediates (e.g., levogalactosan) or byproducts (e.g., FA).

**2.4. Definitions and Determination of the Kinetic Parameters.** The conversion of GAL ($X_{GAL}$) and yields of HMF ($Y_{HMF}$) and LA ($Y_{LA}$) were calculated using eqs 1−3.

$$X_{GAL} = \frac{C_{GAL,0} - C_{GAL}}{C_{GAL,0}} \times 100\% \quad (1)$$

$$Y_{HMF} = \frac{C_{HMF} - C_{HMF,0}}{C_{GAL,0}} \times 100\% \quad (2)$$

$$Y_{LA} = \frac{C_{LA} - C_{LA,0}}{C_{GAL,0}} \times 100\% \quad (3)$$



https://doi.org/10.1021/acs.iecr.2c00706
Ind. Eng. Chem. Res. 2022, 61, 9178−9191

**Table 2. Overview of Kinetic Studies on GAL Degradation**

| scheme | $[C_{GAL}]_0$ | catalyst | conditions | $T$ (°C) | reaction time | kinetic expression | activation energy (kJ·mol$^{-1}$) | Ref |
|---|---|---|---|---|---|---|---|---|
| GAL $\xrightarrow{R_G}$ products | 5 g/100 mL | $C_{H_2SO_4}$= 0.8% | batch system, isothermal operation | 180 | 5−40 min | $R_G = 0.0273[GAL]$[a] | n.a | 18 |
| GAL $\xrightarrow{R_G}$ products | 11.1 mM | buffer solution (0.3 M butyric acid and 0.05 M phosphoric acid); pH = 2.0−4.0 | batch system, isothermal operation | 170, 190, 210 | n.a | $R_G = (7.7 \times 10^{13} + 3.7 \times 10^{24}[OH^-])\exp\left(\frac{-E_G}{RT}\right)[GAL]$[a] | $E_G$ = 138 | 19 |
| GAL $\xrightarrow{R_G}$ products | 0.002 M | $C_{HCl}$ = 0.14−0.41 | batch system, isothermal operation | 120, 130, 140 | 0.75−5.75 h | $R_G = 8.21 \times 10^{17}[HCl]\exp\left(\frac{-E_G}{RT}\right)[GAL]$[b] | $E_G$ = 141.6 | 20 |
| | | $C_{H_2SO_4}$ = 0.20−0.61 | | | 0.75−5.75 h | $R_G = 6.16 \times 10^{18}[H_2SO_4]\exp\left(\frac{-E_G}{RT}\right)[GAL]$[b] | $E_G$ = 147.5 | |
| | | $C_{H_2SO_3}$ = 0.16−0.63 | | | 1.75−13.75 h | $R_G = 4.21 \times 10^{17}[H_2SO_3]\exp\left(\frac{-E_G}{RT}\right)[GAL]$[b] | $E_G$ = 148.3 | |
| polymer $\xrightarrow{R_P}$ GAL $\xrightarrow{R_G}$ products<br>HMF $\xrightarrow{R_H}$ products | douglas fir, liquid-to-solid ratio = 4<br>$C_{HMF}$ = 44.2 g·L$^{-1}$ | 3.34% calcium bisulfite and 1.06% free sulfur dioxide | batch system, isothermal operations | pretreatment: 135, 145, 155; hydrolysis: 50 | pretreatment: 20−180 min; hydrolysis: 0−72 h | $R_P = 2.4 \times 10^9\exp\left(\frac{-E_P}{RT}\right)[polymer]$[c]<br>$R_G = 8.89 \times 10^6\exp\left(\frac{-E_G}{RT}\right)[GAL]$[c]<br>$R_H = 7.22 \times 10^9\exp\left(\frac{-E_H}{RT}\right)[HMF]$[c] | $E_P$ = 93.5<br>$E_G$ = 73.1<br>$E_H$ = 108.9 | 21 |
| GAL $\xrightarrow{R_G}$ products | 0.5% (w/v) | n.a | continuous flow system, pressure of 10 MPa | 180−260 | 12−360 s | $\frac{C}{C_0} = \exp\left[-\left(k_0\exp\left(-\frac{E_G}{RT}\right)\tau\right)^n\right]$ | $E_G$ = 170 | 22 |

[a] $k_G$ in min$^{-1}$,. [b] $R_G$ in mol. L$^{-1}$.h$^{-1}$,. [c] $R_P$, $R_G$, and $R_H$ in g·L$^{-1}$·min$^{-1}$.



https://doi.org/10.1021/acs.iecr.2c00706
Ind. Eng. Chem. Res. 2022, 61, 9178−9191

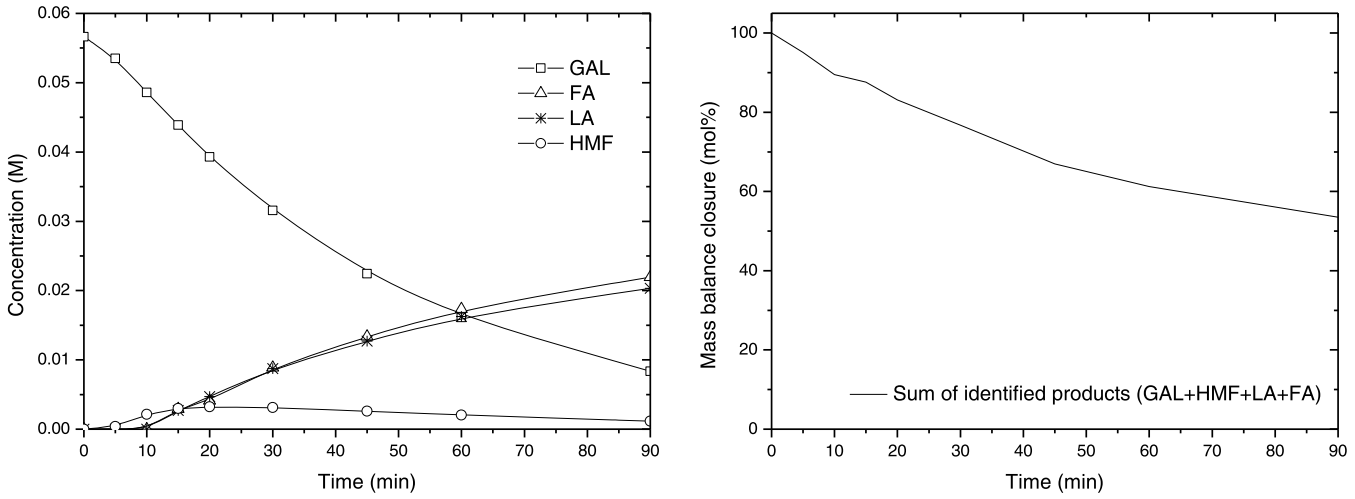


**Figure 2.** Typical concentration profile (left) and the mass balance closure (right) ($T$ = 180 °C, $C_{GAL,0}$ = 0.055 0 M, $C_{H_2SO_4}$ = 0.05 M).

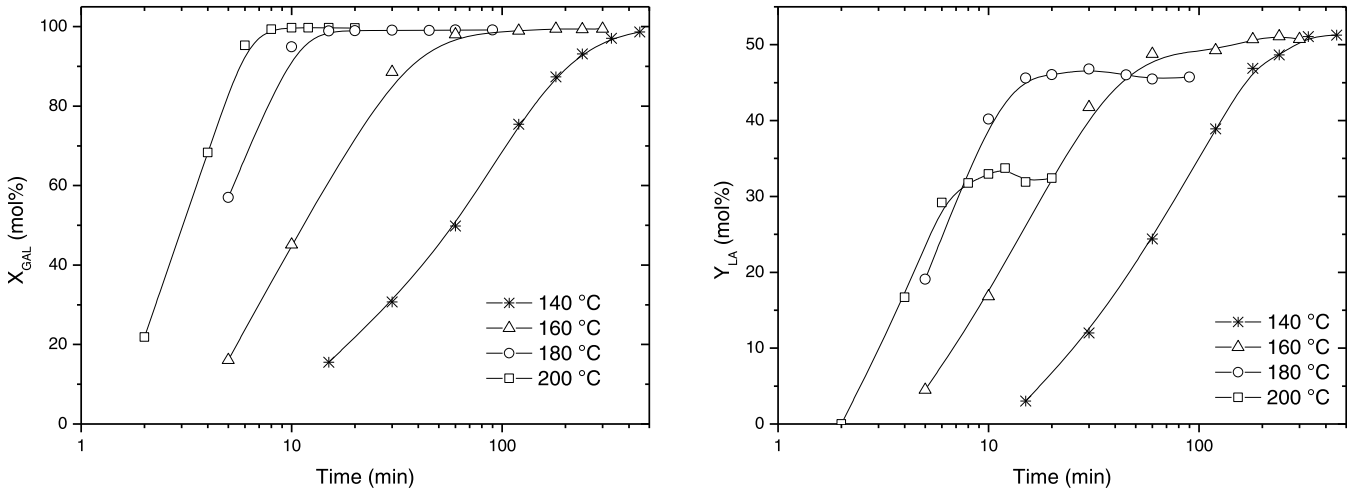


**Figure 3.** Effect of temperature on GAL conversion (left) and yield of LA (right). Conditions: $C_{GAL,0}$ = 0.055 M, $C_{H_2SO_4}$ = 1 M.

Kinetic parameters of the acid-catalyzed hydrolysis of GAL were determined using MATLAB with the lsqnonlin method to minimize the error between experimental data and the model.

## 3. RESULTS AND DISCUSSION

A total of 39 experimental series were performed with temperatures between 140 and 200 °C, initial GAL concentration ($C_{GAL}$) between 0.055 and 1.110 M, and a sulfuric acid concentration between 0.05 and 1 M (see the SI, Table S1). The reproducibility of the experiments was good (see the SI, Figure S3). A typical concentration profile is shown in Figure 2 (left). GAL is converted, and HMF, LA, and FA are formed. The color of the mixture solution changes from colorless to light yellow up to dark brown, which is indicative of the formation of soluble condensation products (humins). In a later stage, the humins become insoluble and black/dark-brown solids are formed.[8] The maximum experimental LA yield was 51 mol % at 140 °C, $C_{GAL}$ = 0.055 M, and $C_{H_2SO_4}$ = 1 M. The maximum HMF yield is low and typically below 10%, which is common when using aldoses as the feed and water as the reaction medium.[3,7−9,13] The highest HMF yield (9 mol %) was achieved at 200 °C, $C_{GAL}$ = 0.055 M, and $C_{H_2SO_4}$ = 0.05 M (see the SI, Section S4).

Mass balance calculations were conducted based on the GAL intake and the total amount of detectable components by HPLC (GAL, HMF, LA, and FA). Mass balance closures are good at the start of the reaction but are significantly reduced at prolonged batch times (Figure 2, right). This is most likely due to the formation of soluble and insoluble oligo- and polymeric condensation products (humins), which cannot be quantified using HPLC. Humin yields ranging from 30 to 39 wt % for various sugars (GLU, FRC, XYL) have been reported in water when using $H_2SO_4$ as the catalyst at 180 °C.[23]

In addition, the HPLC chromatograms (see the SI, Figure S2) also show some additional small peaks. Levogalactosan (1,6-anhydro-$\beta$-D-galactopyranose) was identified and quantified (up to 4 mol %), while 1,6-anhydro-$\alpha$-D-galactofuranose was not detected. The extent of GAL conversion to both anhydrosugars was studied by Angyal et al. at 100 °C in aqueous solutions in the presence of an acidic ion-exchange resin.[24] The amount of anhydrosugars at equilibrium at 100 °C is very low (less than 1 mol %). Moreover, it was shown that the formation of 1,6-anhydro-$\beta$-D-galactopyranose is favored and hardly any 1,6-anhydrofuranose was detected.[24]



https://doi.org/10.1021/acs.iecr.2c00706
Ind. Eng. Chem. Res. 2022, 61, 9178−9191

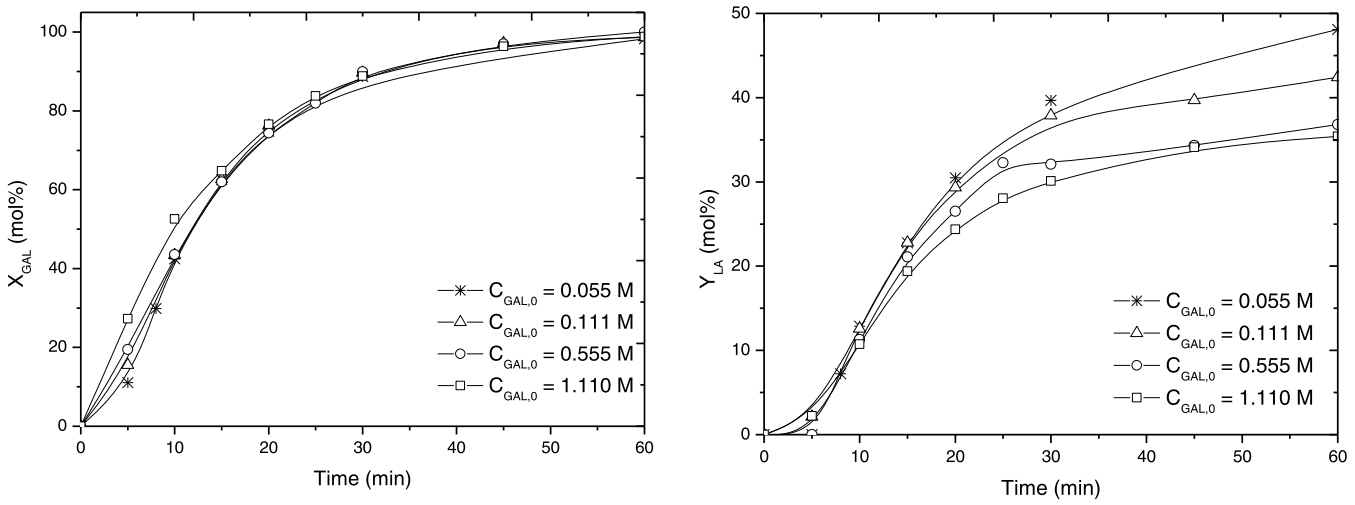


**Figure 4.** Effect of the initial GAL concentration on GAL conversion (left) and yield of LA (right). Conditions: 180 °C, $C_{H_2SO_4}$ = 0.2 M.

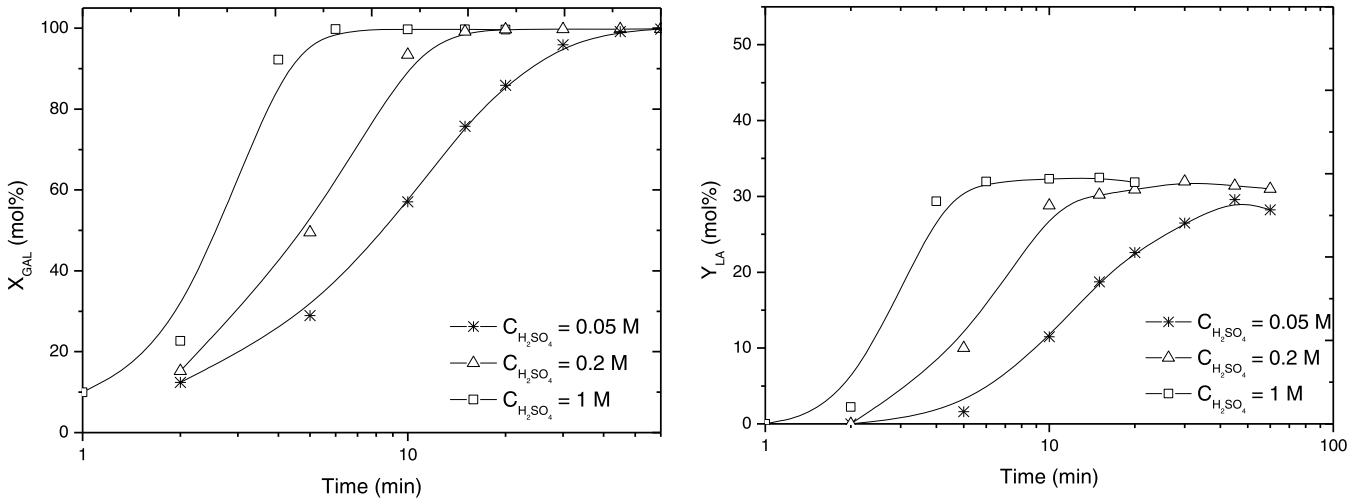


**Figure 5.** Effect of $H_2SO_4$ concentration on GAL conversion (left) and yield of LA (right). Conditions: 200 °C, $C_{GAL,0}$ = 1.110 M.

**Scheme 1. Proposed Reaction Network for the Acid-Catalyzed Reaction of GAL to LA**

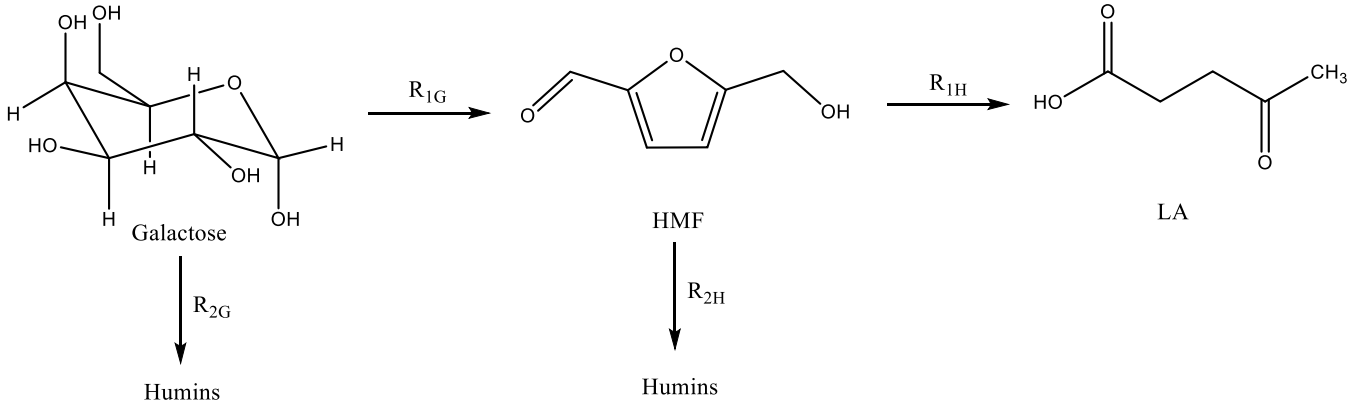


Other possible byproducts are tagatose and 1,3-dihydroxyacetone (DHA). Tagatose is an isomerization product of GAL and is known to be formed in the presence of Lewis acids.[25] However, tagatose could not be detected by HPLC, likely due to a rapid conversion to HMF at the prevailing conditions.[26] DHA was also not detected in the samples, possibly due to rapid successive reactions leading to, among others, organic acids like lactic, acetic, and formic acids.[7,27,28]

**3.1. Effect of Process Variables on GAL Conversion and Yield of LA.** The concentration profiles for GAL and LA show a strong temperature dependency. Quantitative GAL conversion was obtained after 10 min at 200 °C, whereas it takes more than 7.5 h at 140 °C ($C_{GAL,0}$ = 0.055 M, $C_{H_2SO_4}$ = 1



https://doi.org/10.1021/acs.iecr.2c00706
Ind. Eng. Chem. Res. 2022, 61, 9178−9191

Table 3. Kinetic Parameters of the Sulfuric Acid-Catalyzed Hydrolysis of GAL, GLU, and FRC

| parameter | GAL (this research, model 1) | GLU[8] | FRC[66] |
|---|---|---|---|
| $k_{1RG}$ ($M^{1-a_G-\alpha_G}$ $min^{-1}$) | 0.006 ± 0.001 | 0.013 ± 0.001 | 1.1 ± 0.1 |
| $k_{2RG}$ ($M^{1-b_G-\beta_G}$ $min^{-1}$) | 0.008 ± 0.001 | 0.013 ± 0.001 | 0.55 ± 0.1 |
| $E_{1G}$ ($kJ \cdot mol^{-1}$) | 140.2 ± 2.3 | 152.2 ± 0.7 | 123 ± 5 |
| $E_{2G}$ ($kJ \cdot mol^{-1}$) | 123.2 ± 4.0 | 164.7 ± 0.6 | 148 ± 12 |
| $a_G$ | 0.95 ± 0.02 | 1.09 ± 0.01 | 1.006 ± 0.003 |
| $b_G$ | 1.22 ± 0.03 | 1.30 ± 0.02 | 1.179 ± 0.06 |
| $\alpha_G$ | 1.07 ± 0.03 | 1.13 ± 0.01 | 0.958 ± 0.02 |
| $\beta_G$ | 0.82 ± 0.04 | 1.12 ± 0.02 | 1.056 ± 0.06 |
| $k_{1RH}$ ($M^{1-a_H-\alpha_H}$ $min^{-1}$) | 0.166 ± 0.078 | 0.340 ± 0.010 | 0.38 ± 0.04 |
| $k_{2RH}$ ($M^{1-b_H-\beta_H}$ $min^{-1}$) | 0.040 ± 0.034 | 0.117 ± 0.008 | 0.142 ± 0.04 |
| $E_{1H}$ ($kJ \cdot mol^{-1}$) | 78.8 ± 8.5 | 110.5 ± 0.7 | 92 ± 5 |
| $E_{2H}$ ($kJ \cdot mol^{-1}$) | 115.8 ± 12.0 | 111 ± 2.0 | 119 ± 10 |
| $a_H$ | 1.00 ± 0.07 | 0.88 ± 0.01 | 0.89 ± 0.03 |
| $b_H$ | 1.00 ± 0.09 | 1.23 ± 0.03 | 1.21 ± 0.08 |
| $\alpha_H$ | 0.86 ± 0.08 | 1.38 ± 0.02 | 1.16 ± 0.02 |
| $\beta_H$ | 1.13 ± 0.11 | 1.07 ± 0.04 | 0.90 ± 0.05 |

M, Figure 3, left side). The maximum attainable yield of LA is also temperature-dependent, and higher yields are found at lower temperatures (Figure 3, right side).

The effect of the initial GAL concentration was also investigated ($T$ = 180 °C, $C_{H_2SO_4}$ = 0.2 M), and the GAL conversion was found to be independent of the initial GAL concentration (Figure 4, left side). This result indicates that the order in GAL in the kinetic model is close to one. On the contrary, the maximum LA yield is a function of the initial GAL concentration. Higher yields of LA were obtained at lower initial GAL concentrations (Figure 4, right side). These findings indicate that unfavorable side reactions e.g., to humins, are favored at higher GAL concentrations, implying that the order in reactants for these reactions should exceed 1.

An S-shaped curve for conversion versus time is observed in some cases, and this is particularly visible in the left part of Figures 3−5. This is due to the nonisothermal behavior at the start of a hydrolysis reaction due to the heating up of the glass ampoule and its content from room temperature to oven temperature. This effect was compensated for in the kinetic studies by determination of the heating profiles (see the SI Section S5) and subsequent modeling of these profiles (SI, Section S6) using a published procedure.[8]

Acid concentration significantly affects both the reaction rate of GAL and LA formation (Figure 5). For instance, it takes about 5 min to reach 100% GAL conversion and maximum LA yield when using 1 M $H_2SO_4$ versus 45 min at 0.05 M.

**3.2. Kinetic Modeling for the Acid-Catalyzed Conversion of GAL to LA.** The reaction network used as the basis for the kinetic modeling of the sulfuric acid-catalyzed conversion of GAL to LA is given in Scheme 1. It involves the reaction of GAL to HMF, followed by a subsequent reaction of HMF to LA. Humins are formed from either GAL or HMF. This simplified reaction network has also been successfully applied to kinetic studies by our group involving GLU and FRC.[6,8] It does not take into account the formation of reversion products (e.g., anhydrosugars) and other intermediates, rationalized by their low abundance during the reaction (*vide supra*).

The reaction rates for the individual reactions in the network were defined using a power-law approach (eqs 4−7).

$$R_{1G} = k_{1G}(C_{GAL})^{a_G} \tag{4}$$

$$R_{2G} = k_{2G}(C_{GAL})^{b_G} \tag{5}$$

$$R_{1H} = k_{1H}(C_{HMF})^{a_H} \tag{6}$$

$$R_{2H} = k_{2H}(C_{HMF})^{b_H} \tag{7}$$

The temperature dependence of the kinetic constants was introduced using modified Arrhenius equations (eqs 8−11).

$$k_{1G} = (C_{H^+})^{\alpha_G} k_{1RG} \exp^{[E_{1G}/R(T-T_R/T_RT)]} \tag{8}$$

$$k_{2G} = (C_{H^+})^{\beta_G} k_{2RG} \exp^{[E_{2G}/R(T-T_R/T_RT)]} \tag{9}$$

$$k_{1H} = (C_{H^+})^{\alpha_H} k_{1RH} \exp^{[E_{1H}/R(T-T_R/T_RT)]} \tag{10}$$

$$k_{2H} = (C_{H^+})^{\beta_H} k_{2RH} \exp^{[E_{2H}/R(T-T_R/T_RT)]} \tag{11}$$

Here, $T$ is the actual reaction temperature and $T_R$ is the reference temperature (140 °C). At the start of the reaction, the reactor has to heat up to the preset temperature, and this heating-up profile has been incorporated into the model (eq S3 in the SI). The concentration of $H^+$ was calculated using eq 12.

$$C_{H^+} = C_{H_2SO_4} + \frac{1}{2}\left(-(K_{a,HSO_4^-}) + \sqrt{(K_{a,HSO_4^-})^2 + 4(C_{H_2SO_4}K_{a,HSO_4^-})}\right) \tag{12}$$

$K_{a,HSO_4^-}$ in eq 12 represents the dissociation constant of $HSO_4^-$ for which a value of $10^{-3.6}$ was applied.[6,8] The concentrations of GAL, HMF, and LA as a function of time in a batch system are presented by the differential equations given in eqs 13−15.

$$\frac{dC_{GAL}}{dt} = -(R_{1G} + R_{2G}) \tag{13}$$

$$\frac{dC_{HMF}}{dt} = R_{1G} - (R_{1H} + R_{2H}) \tag{14}$$

$$\frac{dC_{LA}}{dt} = R_{1H} \tag{15}$$

A total of 1044 data points (39 experiments, 8−9 samples per experiment, being the concentrations of GAL, HMF, and LA for each sample) were used to develop the kinetic model. The best estimates of the kinetic parameters are shown in Table 3.



https://doi.org/10.1021/acs.iecr.2c00706
Ind. Eng. Chem. Res. 2022, 61, 9178−9191

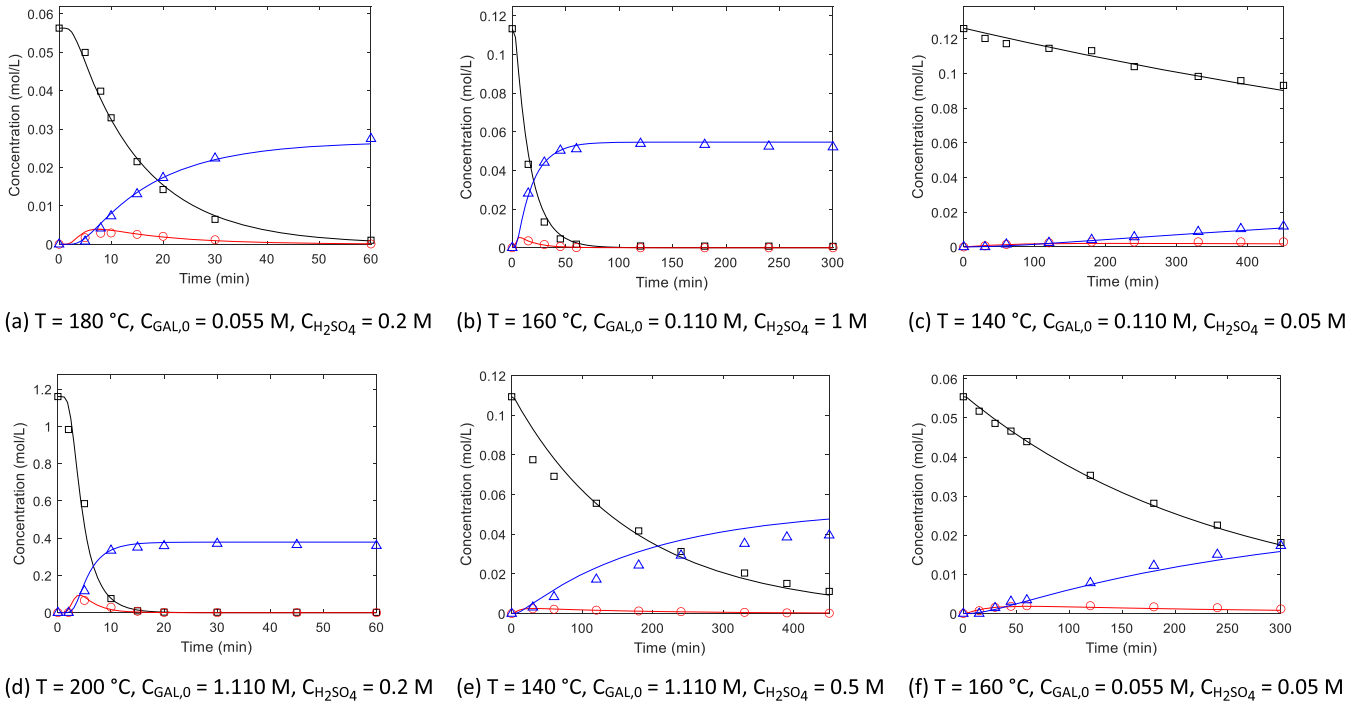


**Figure 6.** Experimental (□: GAL; ○: HMF; Δ: LA) and modeled (solid lines) concentration−time profiles for a number of selected experiments.

In this table, also a comparison with kinetic models for other sugars (GLU, FRC) as reported by us using the same reaction network is provided.

The experimental and modeled (model 1) concentration−time profiles for a number of experiments are given in Figure 6 and shows good agreement between experiments and the model for a broad range of reaction conditions. A parity plot (Figure 7) confirms this and shows the goodness-of-fit between the experimental data and the model.

The activation energy of the reaction of GAL to HMF was estimated at 140.2 ± 2.3 kJ·mol$^{-1}$. It is comparable to the results reported by Shi et al. (147.5 kJ·mol$^{-1}$) using sulfuric acid as the catalyst in the temperature range of 120−140 °C[20] and by Baugh and McCarty (138 kJ·mol$^{-1}$) at 170−210 °C at a pH range of 2.0−4.0.[19] The order in GAL was close to 1 ($a_G$ = 0.95 ± 0.02), in line with the experimental results given in Figure 4 (left side) showing that GAL conversion is essentially independent of the initial GAL concentration. The order in GAL for the reaction to give humins is much higher, viz. 1.22 ± 0.03.

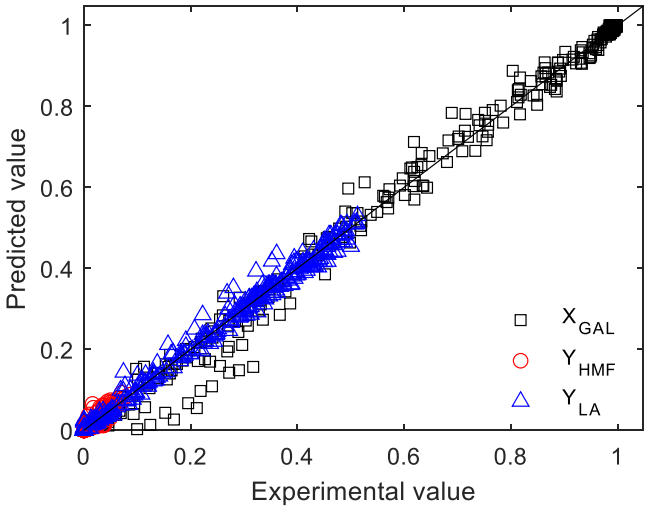


**Figure 7.** Parity plot of experimental and predicted conversion and yield data.

Several models with less kinetic parameters than model 1 have also been tested. The goodness-of-fit approach (eqs 16−18) and the Akaike Information Criterion/AIC (eq 19) was applied to compare the quality of the models. For the latter, $n$ is the number of data points, $\hat{\varepsilon}_i$ are the estimated residuals from the fitted model, and $k$ is the number of parameters in the model. For the AIC criterion, the best model has the lowest value.

$$\%\mathrm{FIT}_{\mathrm{GAL}} = \left[1 - \frac{\mathrm{norm}(C_{\mathrm{GAL}} - \hat{C}_{\mathrm{GAL}})}{\mathrm{norm}(C_{\mathrm{GAL}} - \bar{C}_{\mathrm{GAL}})}\right] \times 100\% \quad (16)$$

$$\%\mathrm{FIT}_{\mathrm{HMF}} = \left[1 - \frac{\mathrm{norm}(C_{\mathrm{HMF}} - \hat{C}_{\mathrm{HMF}})}{\mathrm{norm}(C_{\mathrm{HMF}} - \bar{C}_{\mathrm{HMF}})}\right] \times 100\% \quad (17)$$

$$\%\mathrm{FIT}_{\mathrm{LA}} = \left[1 - \frac{\mathrm{norm}(C_{\mathrm{LA}} - \hat{C}_{\mathrm{LA}})}{\mathrm{norm}(C_{\mathrm{LA}} - \bar{C}_{\mathrm{LA}})}\right] \times 100\% \quad (18)$$

$$\mathrm{AIC} = n \log\left(\frac{\sum \hat{\varepsilon}_i^2}{2}\right) + 2k \quad (19)$$

Model 2 is a model that includes the kinetic parameters for the reaction of HMF to LA and HMF to humins. The latter were taken from a previous study by our group using pure HMF as the feed.[29] As such, only the kinetic parameters for the reaction of GAL to HMF and GAL to humins need to be determined, and this reduces the number of parameters from 16 to 8. The kinetic modeling results using this approach are given in Table 4. The model fit, especially for the HMF yield, was poor. This could be due to the simplicity of the reaction network used



https://doi.org/10.1021/acs.iecr.2c00706
Ind. Eng. Chem. Res. 2022, 61, 9178−9191

Table 4. Comparison of Several Kinetic Models of GAL Conversion to HMF and LA

| parameter | model 1[a] | model 2[b] | model 3[a] | model 4[a] |
|---|---|---|---|---|
| $k_{1RG}$ ($M^{1-a_G-\alpha_G}$ $min^{-1}$) | 0.006 ± 0.001 | 0.005 ± 0.0002 | 0.006 ± 0.0004 | 0.005 ± 0.0002 |
| $k_{2RG}$ ($M^{1-b_G-\beta_G}$ $min^{-1}$) | 0.008 ± 0.001 | 0.008 ± 0.0004 | 0.008 ± 0.001 | 0.006 ± 0.0003 |
| $E_{1G}$ ($kJ \cdot mol^{-1}$) | 140.2 ± 2.3 | 128.4 ± 1.3 | 140.4 ± 2.1 | 137.5 ± 3.8 |
| $E_{2G}$ ($kJ \cdot mol^{-1}$) | 123.2 ± 4.0 | 135.9 ± 1.5 | 123.5 ± 3.2 | 133.0 ± 4.1 |
| $a_G$ | 0.95 ± 0.02 | 0.99 ± 0.01 | 0.96 ± 0.01 | 1 |
| $b_G$ | 1.22 ± 0.03 | 1.14 ± 0.01 | 1.21 ± 0.03 | 1 |
| $\alpha_G$ | 1.07 ± 0.03 | 0.95 ± 0.02 | 1.07 ± 0.03 | 1 |
| $\beta_G$ | 0.82 ± 0.04 | 0.96 ± 0.02 | 0.82 ± 0.04 | 1 |
| $k_{1RH}$ ($M^{1-a_H-\alpha_H}$ $min^{-1}$) | 0.166 ± 0.078 | 0.340 ± 0.010 | 0.176 ± 0.042 | 0.190 ± 0.051 |
| $k_{2RH}$ ($M^{1-b_H-\beta_H}$ $min^{-1}$) | 0.040 ± 0.034 | 0.117 ± 0.008 | 0.039 ± 0.017 | 0.003 ± 0.006 |
| $E_{1H}$ ($kJ \cdot mol^{-1}$) | 78.8 ± 8.5 | 110.5 ± 0.7 | 79.5 ± 7.3 | 82.0 ± 9.2 |
| $E_{2H}$ ($kJ \cdot mol^{-1}$) | 115.8 ± 12.0 | 111.0 ± 2.0 | 119.0 ± 9.8 | 167.2 ± 38.5 |
| $a_H$ | 1.00 ± 0.07 | 0.88 ± 0.01 | 1 | 1 |
| $b_H$ | 1.00 ± 0.09 | 1.23 ± 0.03 | 1 | 1 |
| $\alpha_H$ | 0.86 ± 0.08 | 1.38 ± 0.02 | 0.90 ± 0.07 | 1 |
| $\beta_H$ | 1.13 ± 0.11 | 1.07 ± 0.04 | 1.19 ± 0.10 | 1 |
| $\%FIT_{GAL}$ | 91% | 91% | 91% | 89% |
| $\%FIT_{HMF}$ | 54% | 8% | 56% | 55% |
| $\%FIT_{LA}$ | 90% | 87% | 90% | 80% |
| AIC | −951 | −922 | −954 | −869 |

[a]This research. [b]Kinetic parameters of HMF to LA and HMF to humins were taken from Girisuta et al.[29]

here, which does not consider interactions of the starting sugars with intermediates to form humins. The rates of these reactions may be different for the different sugars used.

Model 3 is a simplified version of model 1, and in this case, the order of HMF for the reaction to LA ($a_H$) and to humins ($b_H$) was set to 1 based on the observation that the estimated model parameters are 1 within the error limits. The goodness-of-fit and the AIC values are marginally better when compared to model 1 although activation energies are similar within the error margins.

Model 4 is a kinetic model where all of the orders in the reactants and acid concentrations for the various reactions in the network are set to 1. This reduces the number of parameters from 16 for model 1 to 8 for model 4. The %FIT and the AIC values for this model are worse than for model 1. Thus, although model 4 is the simplest one, it is not the best one to describe the experimental data. This model discrimination exercise implies that model 3 is the most accurate in terms of goodness-of-fit and AIC and was used in the next paragraphs.

### 3.3. Application of the Kinetic Model (Model 3).

*3.3.1. Batch Simulation and Optimization.* Figure 8 shows the modeled LA yield as a function of temperature and $H_2SO_4$ concentration for model 3. The highest predicted yield of LA (54 mol %) is achieved at intermediate temperatures between 130 and 140 °C at the highest concentration of sulfuric acid (1 M). The experimental yield was about 51 mol % at these conditions. The graph reveals that the optimum LA yield is likely not within the window of operating conditions used in this study and that higher $H_2SO_4$ concentrations may be beneficial.

A typical batch time to obtain 90 mol % GAL conversion as a function of temperature is given in Figure 9. It requires more than 10,000 min to achieve 90 mol % GAL conversion at 100 °C, whereas less than 2 min is required at 200 °C.

The batch time versus temperature profiles for GLU and FRC, as previously determined by our group, are also provided in Figure 9. The profile for GAL shows a strong resemblance to

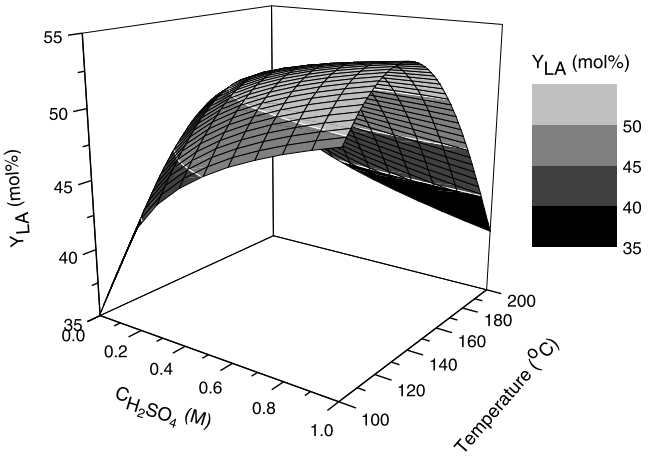


**Figure 8.** Effect of temperature and sulfuric acid concentration on the yield of LA. Conditions: $C_{GAL,0}$ = 0.05 M, $X_{GAL}$ = 100%.

that of GLU. At lower temperatures, GAL is slightly more reactive, which is also represented by the slightly lower activation energy for the reaction of GAL to HMF (140.4 kJ·mol$^{-1}$) compared to that of GLU (152.2 kJ·mol$^{-1}$). Among the three monosaccharides, FRC is by far the most reactive, with shorter batch times to reach 90% conversion at all temperatures.

With the kinetic model available, it is also possible to predict the optimum reaction conditions to achieve the highest selectivity of LA. For this purpose, eq 1 is differentiated to give eq 20.

$$dX_{GAL} = -\frac{dC_{GAL}}{C_{GAL,0}} \tag{20}$$

Combination with eqs 13−15 leads to the differential eqs 21−23. These were solved using the ode45 routine in MATLAB software with the conversion of GAL ranging between 0 and 90 mol %. The selectivity of LA ($\sigma_{LA}$) is defined


https://doi.org/10.1021/acs.iecr.2c00706
Ind. Eng. Chem. Res. 2022, 61, 9178−9191

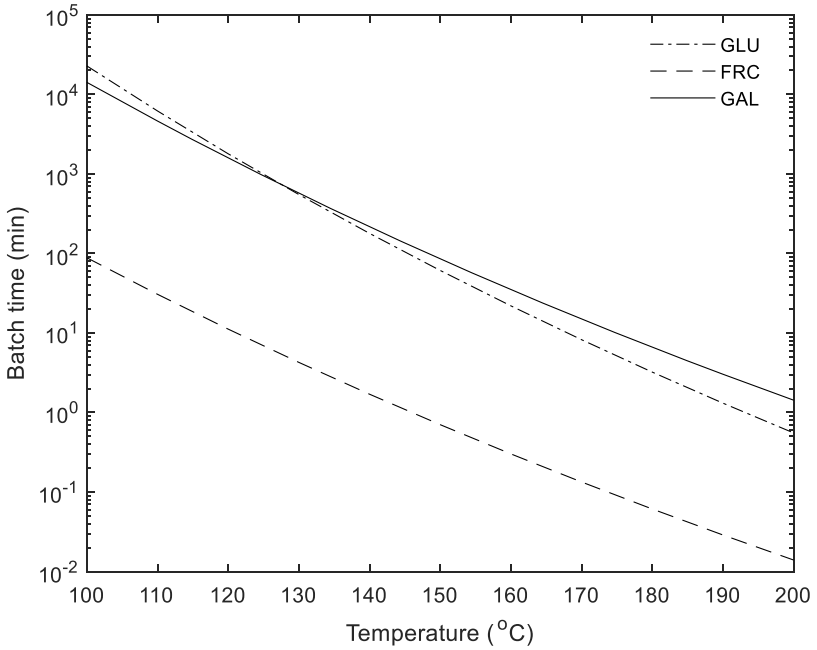


**Figure 9.** Required batch time for 90 mol % conversion of the sugar feed (GLU, FRC, GAL) as a function of the temperature. Conditions: $C_{sugar,0}$ = 0.05 M, $C_{H_2SO_4}$ = 1 M.

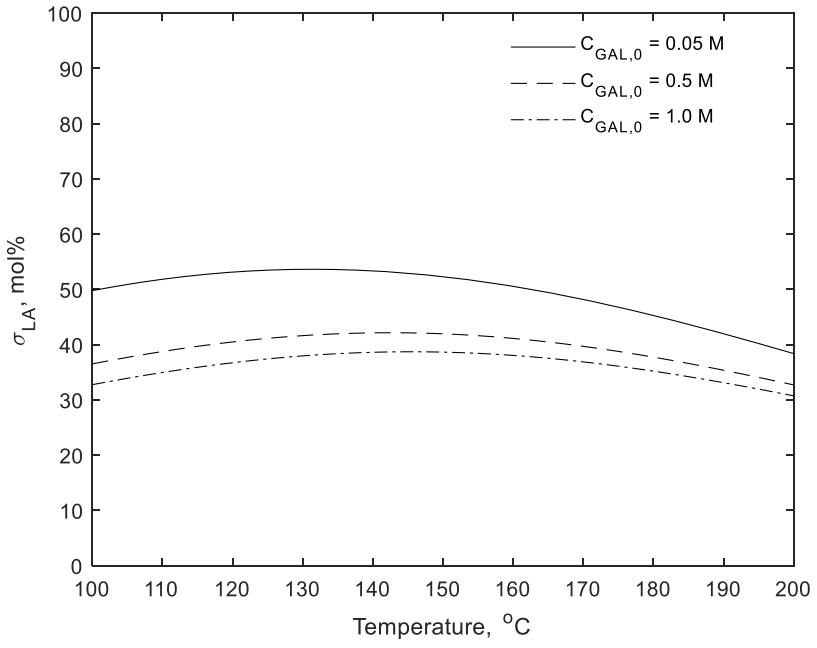


**Figure 10.** Temperature effect on selectivity of LA at $X_{GAL}$ = 90 mol % and $C_{H_2SO_4}$ = 1 M.

as the ratio of the concentration of LA at a certain time and the amount of GAL converted; see eq 24 for details.

$$\frac{dC_{GAL}}{dX_{GAL}} = -C_{GAL,0} \tag{21}$$

$$\frac{dC_{HMF}}{dX_{GAL}} = \frac{R_{1G} - R_{1H} - R_{2H}}{R_{1G} + R_{2G}} C_{GAL,0} \tag{22}$$

$$\frac{dC_{LA}}{dX_{GAL}} = \frac{R_{1H}}{R_{1G} + R_{2G}} C_{GAL,0} \tag{23}$$

$$\sigma_{LA} = \frac{C_{LA} - C_{LA,0}}{C_{GAL,0} - C_{GAL}} = \frac{Y_{LA}}{X_{GAL}} \tag{24}$$

The predicted selectivity of LA as a function of temperature and GAL intake is shown in Figure 10. More dilute GAL solutions result in a higher selectivity of LA. Based on the kinetic model, the orders in GAL for the desired reaction to HMF ($a_G$ = 0.96 ± 0.01) are lower than for the humins forming reaction ($b_G$ = 1.21 ± 0.03). This indicates that a higher concentration of GAL will lead to a reduced selectivity of LA, in line with the experimental results. It is also evident that the selectivity of LA is temperature-dependent. Based on Table 4, the conversion of HMF to LA has the lowest



https://doi.org/10.1021/acs.iecr.2c00706
Ind. Eng. Chem. Res. 2022, 61, 9178−9191

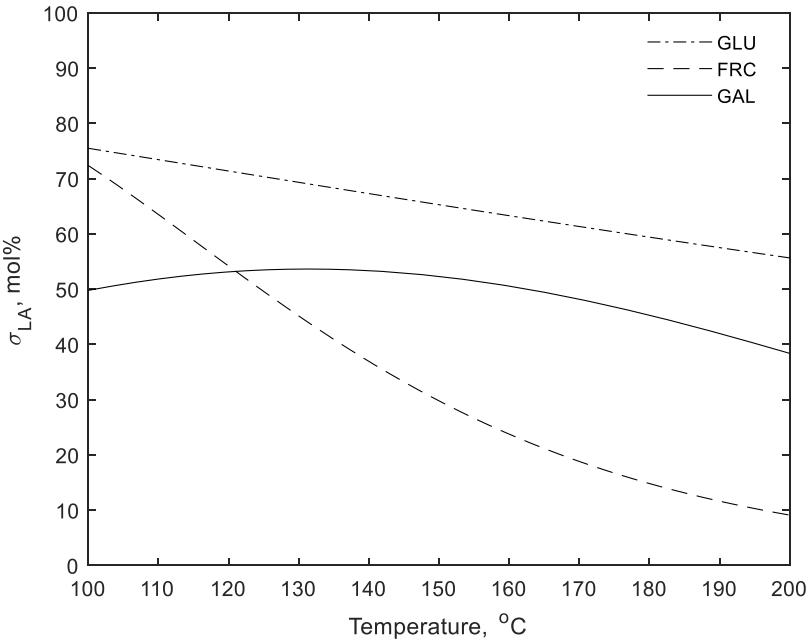


**Figure 11.** Temperature effect on selectivity of LA at $X_{sugar}$ = 90 mol %. Conditions: $C_{sugar,0}$ = 0.05 M, $C_{H_2SO_4}$= 1 M.

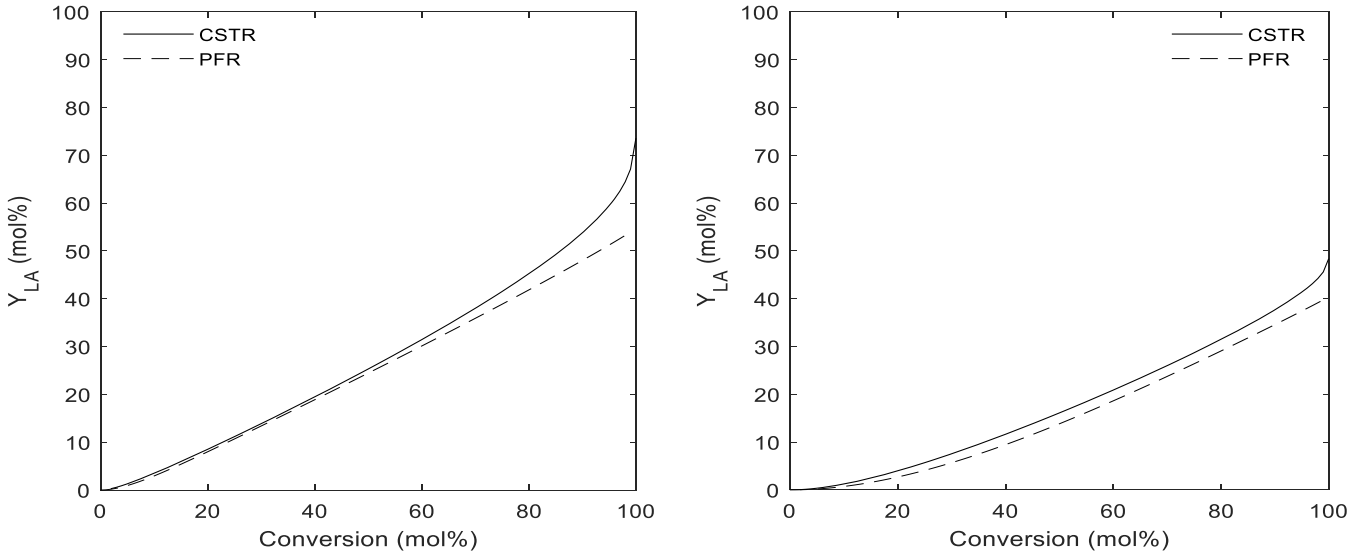


**Figure 12.** Comparisons of LA yield in CISTR and PFR at 140 °C (left side) and 200 °C (right side). Conditions: $C_{GAL,0}$ = 0.05 M, $C_{H_2SO_4}$ = 1 M.

activation energy ($E_{1H}$ = 79.5 kJ mol$^{-1}$), implying that the reaction is favored at a lower temperature.

The LA selectivity versus temperature profile obtained here was compared with data for the conversion of GLU and FRC to LA (Figure 11). Among the three sugars (FRC, GLU, and GAL), GLU gives the highest selectivity of LA within the temperature window evaluated.

*3.3.2. Optimization of LA Yield in Continuous Reactors.* The yield of LA will be a function of process parameters (temperature, initial concentration of GAL, and concentration of sulfuric acid) and the extent of backmixing in continuous reactors. It is possible to model the conversion of GAL and the yield of LA (eq 25) in a plug-flow reactor (PFR) and a continuous ideally stirred-tank reactor (CISTR), two extremes with respect to mixing, with the kinetic model available. The yield and selectivity of LA in the PFR were determined using equations similar to those used for the batch reactor, with the time replaced by the residence time (eqs 20−23). The equations for the CISTR are given in eqs 26−29.

$$Y_{LA} = \frac{C_{LA}^{out} - C_{LA}^{in}}{C_{GAL}^{in}} \tag{25}$$

$$\tau_{CISTR} = \frac{C_i^{out} - C_i^{in}}{R_i} \tag{26}$$

The relation between GAL conversion ($X_{GAL}$) and $\tau_{CISTR}$ is given by eq 27.

$$\tau_{CISTR} = \frac{X_{GAL} - C_{GAL}^{in}}{R_{1G} + R_{2G}} \tag{27}$$

Substituting eq 27 into eq 26 and rearrangement leads to eqs 28 and 29.



https://doi.org/10.1021/acs.iecr.2c00706
Ind. Eng. Chem. Res. 2022, 61, 9178−9191

$$C_{HMF}^{out} = \left(\frac{R_{1G} - R_{1H} - R_{2H}}{R_{1G} + R_{2G}}\right) C_{GAL}^{in} X_{GAL} \quad (28)$$

$$C_{LA}^{out} = \left(\frac{R_{1H}}{R_{1G} + R_{2G}}\right) C_{GAL}^{in} X_{GAL} \quad (29)$$

The yields of LA as a function of GAL conversion at two temperatures (140 and 200 °C) in the PFR and CISTR are provided in Figure 12.

Based on the modeling result shown in Figure 12, it is evident that the LA yield increases with GAL conversion and the yields in the CISTR are higher than in the PFR. Furthermore, the yields are higher at a lower temperature than the yields at high temperatures for both CISTR and PFR configurations.

These findings may be rationalized by considering the orders in reactants. In the case of two parallel reactions with the order of the desired reaction being lower than that of the side reaction, it is better to use a reactor with a high extent of backmixing (CISTR) or a recycle reactor with a high recycle ratio, to maintain the low concentration of the reactant/substrate (dilution effect). In this research, the order of GAL to the desired product ($a_G$ = 0.96) is lower than the order of GAL to humins ($b_G$ = 1.21), implying that backmixing is preferred, which is also in line with the observation that a higher dilution of GAL gives a higher yield of LA (see Figure 4 right).

## 4. CONCLUSIONS

A kinetic model for acid-catalyzed hydrolysis of GAL has been developed for a wide range of process conditions ($C_{GAL,0}$ = 0.055−1.110 M; $C_{H_2SO_4}$ = 0.05−1 M; T = 140−200 °C). Based on the model, the highest yield of LA (54 mol %) was achieved at temperatures 130−140 °C, low initial GAL concentration (0.055 M), and high acid concentration (1 M), which is close to the experimental value. According to the modeling results, the CISTR is the preferable reactor configuration to obtain the highest LA yield. The results of this study are of interest for the development of a full kinetic model for the acid-catalyzed reaction of biomass to levulinic acid in general and of marine biomass in particular. We are currently preparing a kinetic model for the sulfuric acid-catalyzed hydrolysis of κ-carrageenan (the major polysaccharide from red seaweed) to LA in water, using this study as input, and the results will be reported in due course.

## ■ ASSOCIATED CONTENT

### Supporting Information

The Supporting Information is available free of charge at https://pubs.acs.org/doi/10.1021/acs.iecr.2c00706.

Overview of HMF and LA derivatives, typical HPLC chromatogram, experimental data of sulfuric acid-catalyzed hydrolysis of GAL to LA at various conditions, effect of process variables on the yield of HMF, heat-transfer experiments, data and model plot of all experimental series using model 1, and model predictions for HMF and LA yields using model 3 (PDF)

## ■ AUTHOR INFORMATION


### Corresponding Author

**Hero J. Heeres** − *Department of Chemical Engineering (ENTEG), University of Groningen, 9747 AG Groningen, The Netherlands;* orcid.org/0000-0002-1249-543X; Email: h.j.heeres@rug.nl

### Authors

**Angela Martina** − *Department of Chemical Engineering, Parahyangan Catholic University, Bandung 40141, Indonesia; Department of Chemical Engineering (ENTEG), University of Groningen, 9747 AG Groningen, The Netherlands*

**Henk H. van de Bovenkamp** − *Department of Chemical Engineering (ENTEG), University of Groningen, 9747 AG Groningen, The Netherlands*

**Inge W. Noordergraaf** − *Department of Chemical Engineering (ENTEG), University of Groningen, 9747 AG Groningen, The Netherlands*

**Jozef G. M. Winkelman** − *Department of Chemical Engineering (ENTEG), University of Groningen, 9747 AG Groningen, The Netherlands;* orcid.org/0000-0001-7888-1731

**Francesco Picchioni** − *Department of Chemical Engineering (ENTEG), University of Groningen, 9747 AG Groningen, The Netherlands;* orcid.org/0000-0002-8232-2083

Complete contact information is available at: https://pubs.acs.org/10.1021/acs.iecr.2c00706


### Notes

The authors declare no competing financial interest.

## ■ ACKNOWLEDGMENTS

A.M. gratefully acknowledges the Directorate General of Higher Education, Ministry of Education, Culture, Research, and Technology, Indonesia (DIKTI), for funding her Ph.D program. The authors would also like to thank Jan Henk Marsman, Léon Rohrbach, Gert-Jan Boer, Maarten Vervoort, Aad van der Weel, Erwin Wilbers, Marcel de Vries, and Rick van der Reijd for analytical and technical support.

## ■ NOMENCLATURE

| | |
|---|---|
| $a_G$ | reaction order of $C_{GAL}$ in the decomposition of GAL to HMF (−) |
| $\alpha_G$ | reaction order of $C_{H^+}$ in the decomposition of GAL to HMF (−) |
| $a_H$ | reaction order of $C_{HMF}$ in the decomposition of HMF to LA and FA (−) |
| $\alpha_H$ | reaction order of $C_{H^+}$ in the decomposition of HMF to LA and FA (−) |
| $A_t$ | heat-transfer area ($m^2$) |
| $b_G$ | reaction order of $C_{GAL}$ in the decomposition of GAL to humins (−) |
| $\beta_G$ | reaction order of $C_{H^+}$ in the decomposition of GAL to humins (−) |
| $b_H$ | reaction order of $C_{HMF}$ in the decomposition of HMF to humins (−) |
| $\beta_H$ | reaction order of $C_{H^+}$ in the decomposition of HMF to humins (−) |
| $C_{GAL}$ | concentration of GAL (M) |
| $C_{GAL,0}$ | initial concentration of GAL (M) |
| $C_{H^+}$ | concentration of $H^+$ (M) |



https://doi.org/10.1021/acs.iecr.2c00706
Ind. Eng. Chem. Res. 2022, 61, 9178−9191

$C_{H_2SO_4}$ concentration of sulfuric acid (M)
$C_{HMF}$ concentration of HMF (M)
$C_{HMF,0}$ initial concentration of HMF (M)
$C_i^{in}$ concentration of the $i^{th}$ compound at the inflow (M)
$C_i^{in}$ concentration of the $i^{th}$ compound at the outflow (M)
$C_{LA}$ concentration of LA (M)
$C_{LA,0}$ initial concentration of LA (M)
$C_p$ heat capacity of the reaction mixture (J $g^{-1}$ $K^{-1}$)
$E_{1G}$ activation energy of $k_{1G}$ (kJ $mol^{-1}$)
$E_{1H}$ activation energy of $k_{1H}$ (kJ $mol^{-1}$)
$E_{2G}$ activation energy of $k_{2G}$ (kJ $mol^{-1}$)
$E_{2H}$ activation energy of $k_{2H}$ (kJ $mol^{-1}$)
$h$ heat-transfer coefficient from the oven to the reaction mixture ($min^{-1}$)
$k_{1G}$ reaction rate constant of GAL decomposition of HMF ($M^{1-a_G}$ $min^{-1}$)
$k_{1RG}$ reaction rate constant $k_{1G}$ at the reference temperature ($M^{1-a_G-\alpha_G}$ $min^{-1}$)
$k_{1H}$ reaction rate constant of HMF for the main reaction ($M^{1-a_H}$ $min^{-1}$)
$k_{1RH}$ reaction rate constant $k_{1H}$ at the reference temperature ($M^{1-a_H-\alpha_H}$ $min^{-1}$)
$k_{2G}$ reaction rate constant of GAL decomposition of humins ($M^{1-b_G}$ $min^{-1}$)
$k_{2RG}$ reaction rate constant $k_{2G}$ at the reference temperature ($M^{1-b_G-\beta_G}$ $min^{-1}$)
$k_{2H}$ reaction rate constant of HMF for the side reaction to humins ($M^{1-b_H}$ $min^{-1}$)
$k_{2RH}$ reaction rate constant $k_{2H}$ at the reference temperature ($M^{1-b_H-\beta_H}$ $min^{-1}$)
$K_{a,H_2SO_4^-}$ dissociation constant of ($HSO_4-$) (−)
$M$ mass of the reaction mixture (g)
$R$ universal gas constant, 8.314 J $mol^{-1}$ $K^{-1}$
$R_{1G}$ reaction rate of GAL decomposition to HMF (mol $L^{-1}$ $min^{-1}$)
$R_{1H}$ reaction rate of HMF decomposition to LA and FA (mol $L^{-1}$ $min^{-1}$)
$R_{2G}$ reaction rate of GAL decomposition to humins (mol $L^{-1}$ $min^{-1}$)
$R_{2H}$ reaction rate of HMF decomposition to humins (mol $L^{-1}$ $min^{-1}$)
$t$ time (min)
$T$ reaction temperature (°C)
$T_i$ temperature of the reaction mixture at $t$ = 0 (°C)
$T_{oven}$ temperature of the oven (°C)
$T_R$ reference temperature (°C)
$U$ overall heat-transfer coefficient (W $m^{-2}$ $K^{-1}$)
$X_{GAL}$ conversion of GAL (mol %)
$Y_{HMF}$ yield of HMF (mol %)
$Y_{LA}$ yield of LA (mol %)

## GREEK SYMBOLS

$\sigma_{LA}$ selectivity of LA (mol %)
$\tau_{CISTR}$ residence time in a CISTR (min)

## REFERENCES


(1) Signoretto, M.; Taghavi, S.; Ghedini, E.; Menegazzo, F. Catalytic Production of Levulinic Acid (LA) from Actual Biomass. *Molecules* **2019**, *24*, No. 2760.

(2) Stiger-Pouvreau, V.; Bourgougnon, N.; Deslandes, E. *Carbohydrates from Seaweeds*; Elsevier Inc., 2016; pp 223−274 DOI: 10.1016/B978-0-12-802772-1.00008-7.

(3) Van Putten, R. J.; Van Der Waal, J. C.; De Jong, E.; Rasrendra, C. B.; Heeres, H. J.; De Vries, J. G. Hydroxymethylfurfural, a Versatile Platform Chemical Made from Renewable Resources. *Chem. Rev.* **2013**, *113*, 1499−1597.

(4) Hayes, G. C.; Becer, C. R. Levulinic Acid: A Sustainable Platform Chemical for Novel Polymer Architectures. *Polym. Chem.* **2020**, *11*, 4068−4077.

(5) Morone, A.; Apte, M.; Pandey, R. A. Levulinic Acid Production from Renewable Waste Resources: Bottlenecks, Potential Remedies, Advancements and Applications. *Renewable Sustainable Energy Rev.* **2015**, *51*, 548−565.

(6) Fachri, B. A.; Abdilla, R. M.; van de Bovenkamp, H. H.; Rasrendra, C. B.; Heeres, H. J. Experimental and Kinetic Modeling Studies on the Sulfuric Acid Catalyzed Conversion of d -Fructose to 5-Hydroxymethylfurfural and Levulinic Acid in Water. *ACS Sustainable Chem. Eng.* **2015**, *3*, 3024−3034.

(7) Flannelly, T.; Lopes, M.; Kupiainen, L.; Dooley, S.; Leahy, J. J. Non-Stoichiometric Formation of Formic and Levulinic Acids from the Hydrolysis of Biomass Derived Hexose Carbohydrates. *RSC Adv.* **2016**, *6*, 5797−5804.

(8) Girisuta, B.; Janssen, L. P. B. M.; Heeres, H. J. Green Chemicals: A Kinetic Study on the Conversion of Glucose to Levulinic Acid. *Chem. Eng. Res. Des.* **2006**, *84*, 339−349.

(9) Hu, X.; Wu, L.; Wang, Y.; Song, Y.; Mourant, D.; Gunawan, R.; Gholizadeh, M.; Li, C. Z. Acid-Catalyzed Conversion of Mono- and Poly-Sugars into Platform Chemicals: Effects of Molecular Structure of Sugar Substrate. *Bioresour. Technol.* **2013**, *133*, 469−474.

(10) Hu, X.; Jiang, S.; Wu, L.; Wang, S.; Li, C. One-pot Conversion of Biomass-derived Xylose and Furfural into Levulinate Esters via Acid Catalysis. *Chem. Commun.* **2017**, *53*, 2938−2941.

(11) Kim, H. S.; Jeong, G. T. Valorization of Galactose into Levulinic Acid via Acid Catalysis. *Korean J. Chem. Eng.* **2018**, *35*, 2232−2240.

(12) Tuteja, J.; Nishimura, S.; Ebitani, K. One-Pot Synthesis of Furans from Various Saccharides. *Bull. Chem. Soc. Jpn.* **2012**, *85*, 275−281.

(13) Seri, K. I.; Inoue, Y.; Ishida, H. Highly Efficient Catalytic Activity of Lanthanide(III) Ions for Conversion of Saccharides to 5-Hydroxymethyl-2-Furfural in Organic Solvents. *Chem. Lett.* **2000**, *29*, 22−23.

(14) Binder, J. B.; Cefali, A. V.; Blank, J. J.; Raines, R. T. Mechanistic Insights on the Conversion of Sugars into 5- Hydroxymethylfurfural. *Energy Environ. Sci.* **2010**, *3*, 765−771.

(15) Shi, J.; Liu, W.; Wang, N.; Yang, Y.; Wang, H. Production of 5-Hydroxymethylfurfural from Mono- and Disaccharides in the Presence of Ionic Liquids. *Catal. Lett.* **2014**, *144*, 252−260.

(16) Jung, D.; Körner, P.; Kruse, A. Kinetic Study on the Impact of Acidity and Acid Concentration on the Formation of 5-Hydroxymethylfurfural (HMF), Humins, and Levulinic Acid in the Hydrothermal Conversion of Fructose. *Biomass Conv. Bioref.* **2021**, *11*, 1155−1170.

(17) Chang, C.; Ma, X.; Cen, P. Kinetics of Levulinic Acid Formation from Glucose Decomposition at High Temperature. *Chin. J. Chem. Eng.* **2006**, *14*, 708−712.

(18) Saeman, J. F. Kinetics of Wood Saccharification - Hydrolysis of Cellulose and Decomposition of Sugars in Dilute Acid at High Temperature. *Ind. Eng. Chem.* **1945**, *37*, 43−52.

(19) Baugh, K. D.; McCarty, P. L. Thermochemical Pretreatment of Lignocellulose to Enhance Methane Fermentation: I. Monosaccharide and Furfurals Hydrothermal Decomposition and Product Formation Rates. *Biotechnol. Bioeng.* **1988**, *31*, 50−61.

(20) Shi, Y.; Yokoyama, T.; Akiyama, T.; Yashiro, M.; Matsumoto, Y. Degradation Kinetics of Monosaccharides in Hydrochloric, Sulfuric, and Sulfurous Acid. *BioResources* **2012**, *7*, 4085−4097.

(21) Liu, Y.; Wang, J.; Wolcott, M. Modeling the Production of Sugar and Byproducts from Acid Bisulfite Pretreatment and Enzymatic Hydrolysis of Douglas-Fir. *Bioresour. Technol.* **2017**, *224*, 389−396.




https://doi.org/10.1021/acs.iecr.2c00706
*Ind. Eng. Chem. Res.* 2022, 61, 9178−9191

(22) Khajavi, S. H.; Kimura, Y.; Oomori, T.; Matsuno, R.; Adachi, S. Degradation Kinetics of Monosaccharides in Subcritical Water. *J. Food Eng.* **2005**, *68*, 309−313.
(23) Van Zandvoort, I.; Wang, Y.; Rasrendra, C. B.; Van Eck, E. R. H.; Bruijnincx, P. C. A.; Heeres, H. J.; Weckhuysen, B. M. Formation, Molecular Structure, and Morphology of Humins in Biomass Conversion: Influence of Feedstock and Processing Conditions. *ChemSusChem* **2013**, *6*, 1745−1758.
(24) Angyal, S. J.; Dawes, K. Conformational Analysis in Carbohydrate Chemistry. II. Equlibria between Reducing Sugars and Their Glycosidic Anhydrides. *Aust. J. Chem.* **1968**, *21*, 2747−2760.
(25) Drabo, P.; Delidovich, I. Catalytic Isomerization of Galactose into Tagatose in the Presence of Bases and Lewis Acids. *Catal. Commun.* **2018**, *107*, 24−28.
(26) van Putten, R. J.; van der Waal, J. C.; de Jong, E.; Heeres, H. J. Reactivity Studies in Water on the Acid-Catalysed Dehydration of Psicose Compared to Other Ketohexoses into 5-Hydroxymethylfurfural. *Carbohydr. Res.* **2017**, *446*−*447*, 1−6.
(27) Rasrendra, C. B.; Fachri, B. A.; Makertihartha, I. G. B. N.; Adisasmito, S.; Heeres, H. J. Catalytic Conversion of Dihydroxyacetone to Lactic Acid Using Metal Salts in Water. *ChemSusChem* **2011**, *4*, 768−777.
(28) Lux, S.; Siebenhofer, M. Catalytic Conversion of Dihydroxyacetone to Lactic Acid with Brønsted Acids and Multivalent Metal Ions. *Chem. Biochem. Eng. Q.* **2016**, *29*, 575−585.
(29) Girisuta, B.; Janssen, L. P. B. M.; Heeres, H. J. A Kinetic Study on the Decomposition of 5-Hydroxymethylfurfural into Levulinic Acid. *Green Chem.* **2006**, *8*, 701−709.





https://doi.org/10.1021/acs.iecr.2c00706
*Ind. Eng. Chem. Res.* 2022, 61, 9178−9191